J. Min. Metall. Sect. B-Metall. 53 (3) B (2017) 215 - 222

Journal of Mining and Metallurgy, Section B: Metallurgy

PHASE EQUILIBRIA IN THE TERNARY Ag-Au-Ga SYSTEM: ISOTHERMAL SECTIONS AT 250°C AND 450°C

D. Jendrzejczyk-Handzlik

AGH University of Science and Technology, Faculty of Non-Ferrous Metals, Krakow, Poland

(Received 31 May 2017; accepted 26 September 2017)

Abstract

The ternary Ag-Au-Ga system seems to be interesting in jeweller's craft as a joint. Moreover, the ternary systems based on gold and silver have found applications in the dental industry.
A literature overview of the Ag-Au-Ga system shows that the information about phase equilibria of this system does not exist. In the present work, phase equilibria in the Ag-Au-Ga ternary system have been studied by using scanning electron microscopy (SEM) with energy dispersive spectroscopy (EDS) analysis and X-ray diffraction analysis (XRD). Twenty two annealed alloys in the 10-70 at.% Ga region have been investigated. Obtained experimental results were compared with the predicted isothermal sections at two temperatures (250 °C and 450 °C). No ternary compounds are found.

Keywords: *Ag-Au-Ga system; Phase equilibria; Scanning electron microscopy; X-ray diffraction*

1. Introduction

A large variety of hand-made goods from silver and gold has been known since the ancient times. Recently, to push up the price of gold items, different colors of gold were introduced by addition of various alloying elements [1-6]. Special colors of gold like purple, blue, or brown can be obtained using alloys with indium, gallium and aluminum [7-8]. However, thanks to its high electrical conductivity and anticorrosion properties, silver and gold has been also used in interconnections applied in modern electronics industry. Gallium is very interesting metal because its melting temperature is close to the room temperature (302 K), while its evaporation temperature is very high and it is equal to 2073 K. It was shown that the introduction of gallium into multi-component alloys can decrease their melting temperature and facilitate the formation of proper interconnections between high melting transition metals [9]. Gallium has excellent wetting properties [10]. From this point of view, the ternary Ag-Au-Ga system seems to be interesting since this alloy can be used in jeweller's craft as a joint.

Moreover, alloys containing gallium may find more interesting applications. Mouani et al. [11] studied Au-Ga-Te system because tellurium alloys exhibit interesting optical properties. The Cu–In–Ga–Se system is applied in photovoltaics [12] (CIGS) and Cu–Ga–N is semiconductor system [13]. The amalgam solder is an interesting variant of isothermal solidification. It is already successfully applied for electronic interconnections by McKay [14]. In this method, gallium seems to be a suitable candidate for a solvent. Schmid–Fetzer [9] suggested that Ga-based amalgams with metals like Mo, V and even transition metals like Hf, Nb and Zr can be used for soldering in high temperature applications. Consequently, gallium alloys can still be of industrial interest and the thermodynamic database of gallium alloys needs to be created for future predictions of phase equilibria. Moreover, gallium is applied in shape memory alloys. The ternary Ga-Mn-Ni alloys exhibit the giant magneto-mechanical effect [15,16], which allows magnetic-field controlled actuators materials be developed. Unexpectedly, the first shape memory effect was observed in the binary gold-cadmium alloys [17]. This effect in gold can be used for gripping jewels in mounts during jewelry manufacturing.

In the case of the ternary Ag-Au-Ga system, the information about its properties is missing in the monographs of Villars et al. [18] and Petzow and Effenberg [19]. In the literature one can find only two experimental works related to this ternary system. First one, of Andronov et al. [10] is providing the information about wettability of the Ag-Au-Ga thin films. Consequently, the ternary Ag-Au-Ga system

Dedicated to the memory of Professor Dragana Živković

* *Corresponding author: djendrze@agh.edu.pl*

DOI:10.2298/JMMB170531043J

was studied as one of those which can be applied as a solder. The other one, published by Jendrzejczyk-Handzlik [20] reported the results of calorimetric measurements of the enthalpy of mixing at two temperatures 1223 and 1323 K. Results obtained in that experimental work showed that the enthalpy of mixing in this ternary system does not have a temperature dependence. New experimental data are needed to enlarge our knowledge of the phase diagram and melting behaviour of the Ag-Au-Ga system. In this study, phase equilibria in the ternary Ag-Au-Ga system have been established for two isothermal sections at 250 ℃ and 450 ℃ to gain a better knowledge of this ternary system.

2. Constituent Binary Systems

Binary systems: Ag-Au, Ag-Ga and Au-Ga were previously investigated, and Table 1 summarizes information about the phases present in these systems.

2.1 Ag-Au system

Hassam et al. [21] assessed the thermodynamic parameters of the Ag-Au binary system. The Ag-Au phase diagram exhibits a continuous solution both in the liquid and in the solid state that has no intermetallic compounds. The binary Ag-Au system includes 2 phases: liquid and FCC_A1 (Ag, Au). The description of the crystal structures is given in Table 1.

Table 1. *Information on phases in the constituent binary systems according to the literature.*

Phase	Strukturbericht designation	Pearson symbol	Space group
FCC_A1 (Ag, Au, Ga)	A1	cF4	$Fm\bar{3}m$
ζ (HCP_A3)	A3	hP2	$P6_3/mmc$
ζ'(HCP_ORD)	C22	hP9	$P\bar{6}2m$
Ag_3Ga_2	…	…	*Pmmm*
Orthorhombic_GA (Ga)	A11	oC8	*Cmca*
αAu_7Ga	D024	hP16	$P6_3/mmc$
βAu_7Ga_2	...	*(a)*	…
$\beta' Au_7Ga_2$	...	*(b)*	…
γAu_7Ga_3	...	*(b)*	…
AuGa	B31	oP8	*Pnma*
$AuGa_2$	C1	cF12	$Fm\bar{3}m$

(a) Hexagonal; (b) Orthorhombic

2.2 Ag-Ga system

In literature are three independent assessments. First, Okamoto [22] adopted in his assessment Feschotte and Bass [23] results in which they described AgGa phase. Next Zhang et. al [24] have reported the existence of Ag_3Ga_2 instead of AgGa. Zhang et al. [25] carried out the thermodynamic optimization of the Ag–Ga system taking into account a number of different studies. Finally, Gierlotka and Jendrzejczyk-Handzlik [26] re-optimized this binary system considering a large number of phase diagram and thermodynamic data. The information about the Ag-Ga phase diagram are taken from this work. The binary Ag-Ga system includes 6 phases: FCC_A1 (Ag, Ga), Orthorhombic_GA (Ga), ζ (HCP_A3), ζ' (HCP_ORD), Ag_3Ga_2 and liquid. The description of the crystal structures is given in Table 1. The system shows 3 invariant reactions: eutectic reaction between liquid, solid Ga and intermetallic compound Ag_3Ga_2 at temperature 299 K and 2 peritectic reactions: one between Ag, liquid and z phase at 886 K and another between liquid, Ag_3Ga_2 and ζ' at 575 K. The temperature of the order–disorder transformation of the HCP phase is 708 K [27].

2.3 Au-Ga system

The phase diagram has been well established since several experimental studies, assessments and thermodynamic optimization were published. Weibke and Hesse [28] investigated firstly the phase diagram of the Au-Ga system by means of thermal analysis, microscopy and X-ray methods. The new phase αAu_7Ga was detected and confirmed as a hexagonal structure of Ni_3Ti type by Cooke and Hume-Rothery [29]. The available crystallographic data, phase equilibria and thermodynamic data of the Au-Ga binary system were reviewed by Elliot and Shunk [30] and Massalski and Okamoto [31] up to 1983. Recently, in the literature, three independent thermodynamic assessments of this binary system can be found, in which numerous thermodynamic and phase diagram data were taken into account. In all of them, the binary Au-Ga system was assessed by using CALPHAD method. The main difference is found in the description of following intermetallic phases: αAu_7Ga, βAu_7Ga_2, $\beta' Au_7Ga_2$, γAu_7Ga_3. First, Liu et al. [32] have reported intermetallic compounds αAu_7Ga, βAu_7Ga_2, $\beta' Au_7Ga_2$, γAu_7Ga_3, $\gamma' Au_7Ga_3$ which have homogeneity ranges. They were described using a two-sublattice model with Au and Ga or Au on the first sublatice, Au and Ga or Ga on the second one. Next, Wang et al. [33] used substitutional solution model in description of phase αAu_7Ga. The phases βAu_7Ga_2, $\beta' Au_7Ga_2$, γAu_7Ga_3 were described as intermetallic compounds which are treated as stoichiometric compounds (Au_aGa_b) because of their narrow homogeneity ranges determined by Cooke and Hume-Rothery [29, 34]. Recently re-optimization of the Au-Ga system was carried out by Jendrzejczyk-Handzlik [35]. In this

paper, new values of gallium activity in the liquid phase and thermal analysis results (temperatures of liquidus and invariant reactions) were presented. Next, these data were taken into account in optimization of this binary system. The Au-Ga system includes 9 phases: FCC_A1 (Au, Ga), Orthorhombic_GA (Ga), αAu_7Ga and liquid which were described by using substitutional solution model and five line compounds: βAu_7Ga_2, $\beta' Au_7Ga_2$, γAu_7Ga_3, AuGa, $AuGa_2$. The description of the crystal structures is given in Table 1. The system shows 12 invariant reactions: 4 eutectic, 3 peritectic, 2 eutectoid and 2 congruent.

3. Experimental

To analyze the phase equilibria present in the Ag-Au-Ga ternary system, 22 different alloy compositions were made. Table 2 lists the nominal alloy compositions measured in this study and annealing temperatures in the Ag-Au-Ga ternary system.

All ternary alloys were prepared from pure elements: Au (99.99 mass.% from Polish National Mint), Ag (99.999 mass.% from Alfa Aesar, Germany) and Ga (99.99 mass.% from Alfa Aesar, Germany). Twenty two samples (total mass about 0.50 g) were melted in evacuated quartz tubes. After alloying, the samples were homogenized in a two separately operating furnaces at 1200 °C for 10 h. Then, they were annealed in furnace (Linn High Therm VMK 10) at 250 °C (samples 1-10) and 450 °C (samples 11-22) by 8 weeks to form equilibrium phases. After the equilibrium treatment, the tubes were quenched in cold water. The quenched ternary alloys were included into the conductive resin and polished with diamond abrasive spray down to 1 mm grain size. Microstructures of the alloys were systematically investigated by light optical microscopy (Nikon Eclipse LV150). A thorough investigation of each sample by using a scanning electron microscopy (Hitachi SU-70) in back-scattered mode (BSE) in order to reveal the compositional contrast between the different phases was done. All samples were studied by point and region analyses using EDS analysis (Thermo Scientific) attached to the SEM to obtain chemical composition of the phases. The point analyses were performed over five points or areas in each phase. Data acquisition and calculations of chemical composition were done by using NSS 3 software. Generally for each element an error within 0.2 at.% was ascribed. After investigation of microstructure, each sample was subjected to x-ray diffraction (XRD, Rigaku, Mini Flex II) using monochromatic Cu Kα radiation (0.15416 nm). XRD spectra were solved by using PDXL software (Rigaku) with ICDD PDF 2+ Release 2010 database.

4. Results

The equilibrium phases were identified at 250 °C and 450 °C by means of SEM/EDS and XRD analysis. Purpose of prepared samples is to find the new ternary phase in this metallic system. The compositions of the 22 prepared Ag-Au-Ga alloys are reported in Table 2, ordered with increasing at.% of Ga, together with the phases observed for each sample after the annealing at 250 and 450 °C. Three alloys 1, 11 and 12 are with constant amount of Ga 10 at.%. Next, the alloys 2, 13 and 14 with constant amount of Ga 15 at.%. and two alloys 15 and 16 with constant amount of Ga 20 at.%. Three alloys 4, 5 and 20 with constant amount of Ga 40 at.%. Two alloys 17 and 18 are with constant amount of Ga 30 at.%, alloys 7 and 8 with constant amount of Ga 50 at.%, and two alloys 9, 22 with constant amount of Ga 60 at.%. In 4 alloys the amount of Ga was in range from 33.3 to 70 at.%.

4.1 Phase equilibria in the Ag-Au-Ga ternary system

For the experimental investigations of the equilibrium phases present in the ternary Ag-Au-Ga system at two chosen temperatures, the 22 different alloy compositions were prepared. All samples were investigated with SEM/EDS and XRD analysis. According to the present results, no ternary compounds have been found in the Ag-Au-Ga system, so far only binary and unary phases exist in this system having insignificant solubility of the respective third element except a phase.

As a results of the EDS analysis of phase compositions, which correspond to the following phases have been determined, namely: α (complete solid solution between Ag and Au with limited solubility of Ga), AuGa, $AuGa_2$, ζ' (HCP_ORD), Ag_3Ga_2 and liquid. Based on all microstructures of ternary alloys which were detected, one phase is observed in samples 1, 11, 12, 20 and 21. The two-phase equilibria are observed in samples 2-4, 13-19 and 22. Three-phase equilibria are found in samples 5-10. The microstructures of chosen alloys 3-6, 17 and 22 are shown in Fig. 1.

As shown in Fig. 1 two-phase equilibrium was observed in microstructures of samples 3, 4, 17 and 22. While, a three-phase equilibrium was observed in sample 5 and 6. Intermetallic compounds AuGa and $AuGa_2$ are detected as a grey phase. Compound AuGa was observed in microstructures of samples 2 and 5. Compound $AuGa_2$ was observed in samples 4, 5, 6 and 22. The ζ' phase is detected as a dark phase and it is observed in microstructures of samples 4 and 6. The detected solubility of Ga in ζ' phase was 29.7 at.% (sample 4) and 28.8 at.% (sample 6). The a phase was observed in microstructures of samples 3, 5, 6 and 17.

It is a dark grey phase with a detected solubility of Ga 13 at.% (sample 3), 17.8 at.% (sample 5), 18.1 at.% (sample 6) and 20.1 at% (sample 17). Liquid phase with composition $Ag_{26.3}Au_{29.0}Ga_{44.7}$ at.% (sample17) and $Ag_{18.8}Au_{27.0}Ga_{54.2}$ at.% (sample 22) is trapped between grain of a phase in sample 17 and between grain of $AuGa_2$ phase in sample 22. Next, the results of the scanning electron microscopy are also confirmed by the XRD analysis. In Fig. 2 are shown XRD spectra of chosen ternary Ag-Au-Ga alloys.

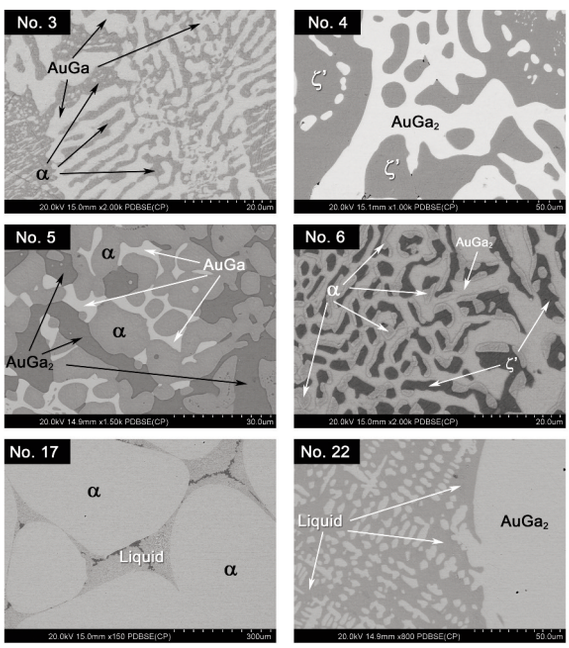

Figure 1. *SEM micrographs (BSE mode) of the six selected alloy samples annealed at 250 °C (samples 3-6) and 450 °C (samples 17 and 22).*

Results of the composition and phase analysis based on SEM/EDS and XRD data of samples annealed at 250 °C and 450 °C are summarized in Table 2. Experimentally determined deviations in chemical composition of the phases are also given in Table 2. The deviations in chemical composition for stoichiometric compounds are within 0.3 at.%, maximal calculated values are for liquid phase and are within 3.1 at. % (alloy no. 9).

4.2 Isothermal sections

Prediction of ternary Ag-Au-Ga system, which was done by using Pandat 8.1 software [36] is compared with experimental data obtained in this work. This prediction is based on information from assessments of binary systems: Ag-Au [21], Ag-Ga [26] and Au-Ga [35]. The binary thermodynamic parameters used for the prediction of phase equilibria in the ternary Ag-Au-Ga system are listed in Table 3.

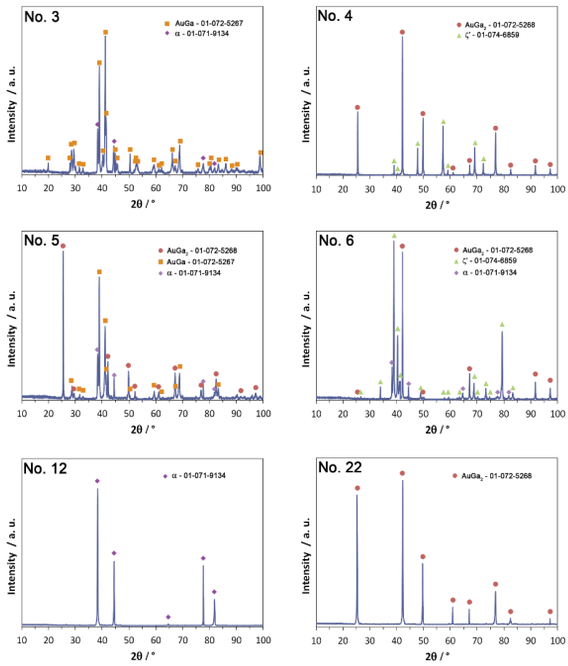

Figure 2. *XRD spectrum of the selected alloy samples annealed at 250 ° C (samples 3-6) and 450 °C (samples 12 and 22).*

The predicted isothermal section at 250 °C compared with experimental results from this work is shown in Fig. 3. On the basis of results presented in Table 2 the following fields are determined: three-phase regions [α+AuGa+$AuGa_2$, α+$AuGa_2$+ζ', $AuGa_2$+Ag_3Ga_2+liquid], two-phase regions [α+AuGa, $AuGa_2$+ζ'] and one-phase region α. The solubility of third element in the binary phases is negligible, except for solid solubility of 18.1 at.% of Ga in α phase.

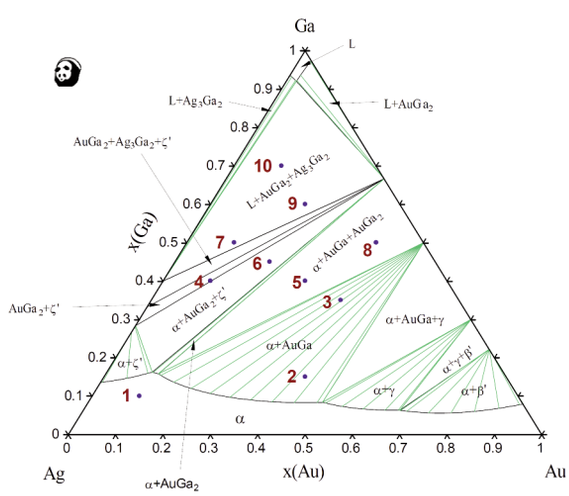

Figure 3. *Predicted isothermal section in the Ag-Au-Ga ternary system at 250 °C compared with experimental results from this work.*

Table 2. *Experimentally determined phases compositions in the ternary Ag-Au-Ga system.*

Alloy No.	Nominal composition / at. %	Anneal. temp. /°C	Theor. predicted phases	Experimentally determined phases		Phase composition determined by EDS / at. %		
				XRD	SEM/EDS	Ag	Au	Ga
1	$Ag_{80}Au_{10}Ga_{10}$	250	α	α	α	80.1 ± 1.0	10.2 ± 0.5	9.7 ± 0.5
2	$Ag_{42.5}Au_{42.5}Ga_{15}$	250	α	α	α	50.4 ± 0.4	40.5 ± 0.6	9.1 ± 0.5
			AuGa	AuGa	AuGa	-	50.3 ± 0.3	49.7 ± 0.3
3	$Ag_{25}Au_{40}Ga_{35}$	250	α	α	α	63.9 ± 0.3	23.1 ± 0.2	13.0 ± 0.3
			AuGa	AuGa	AuGa	-	50.2 ± 0.3	49.8 ± 0.3
4	$Ag_{50}Au_{10}Ga_{40}$	250	$AuGa_2$	$AuGa_2$	$AuGa_2$	-	33.2 ± 0.1	66.8 ± 0.1
			ζ'	ζ'	ζ'	70.3 ± 0.6	-	29.7 ± 0.6
5	$Ag_{30}Au_{30}Ga_{40}$	250	α	α	α	70.1 ± 0.5	12.1 ± 0.6	17.8 ± 0.5
			AuGa	AuGa	AuGa	-	49.9 ± 0.2	50.1 ± 0.2
			$AuGa_2$	$AuGa_2$	$AuGa_2$	-	33.1 ± 0.1	66.9 ± 0.1
6	$Ag_{35}Au_{20}Ga_{45}$	250	α	α	α	71.8 ± 0.6	10.1 ± 0.3	18.1 ± 0.3
			$AuGa_2$	$AuGa_2$	$AuGa_2$	-	33.3 ± 0.1	66.7 ± 0.1
			ζ'	ζ'	ζ'	71.2 ± 0.3	-	28.8 ± 0.3
7	$Ag_{40}Au_{10}Ga_{50}$	250	$AuGa_2$	$AuGa_2$	$AuGa_2$	-	33.0 ± 0.6	67.0 ± 0.6
			Ag_3Ga_2	Ag_3Ga_2	Ag_3Ga_2	60.4 ± 0.4	-	39.6 ± 0.4
			Liquid		Liquid	8.4 ± 2.6	3.5 ± 1.1	88.1 ± 1.4
8	$Ag_{10}Au_{40}Ga_{50}$	250	α	α	α	70.8 ± 1.2	11.9 ± 0.3	17.3 ± 1.1
			AuGa	AuGa	AuGa	-	49.7 ± 0.2	50.3 ± 0.2
			$AuGa_2$	$AuGa_2$	$AuGa_2$	-	33.5 ± 0.4	66.5 ± 0.4
9	$Ag_{20}Au_{20}Ga_{60}$	250	$AuGa_2$	$AuGa_2$	$AuGa_2$	-	33.2 ± 0.4	66.8 ± 0.4
			Ag_3Ga_2	Ag_3Ga_2	Ag_3Ga_2	60.3 ± 0.6	-	39.7 ± 0.6
			Liquid		Liquid	6.8 ± 2.6	3.9 ± 1.8	89.3 ± 3.1
10	$Ag_{20}Au_{10}Ga_{70}$	250	$AuGa_2$	$AuGa_2$	$AuGa_2$	-	32.9 ± 0.7	67.1 ± 0.7
			Ag_3Ga_2	Ag_3Ga_2	Ag_3Ga_2	60.4 ± 0.5	-	39.6 ± 0.5
			Liquid		Liquid	6.4 ± 1.3	2.5 ± 0.2	91.1 ± 1.1
11	$Ag_{80}Au_{10}Ga_{10}$	450	α	α	α	80.2 ± 0.9	9.7 ± 0.4	10.1 ± 0.4
12	$Ag_{60}Au_{30}Ga_{10}$	450	α	α	α	59.7 ± 1.0	30.6 ± 0.4	9.7 ± 0.7
13	$Ag_{42.5}Au_{42.5}Ga_{15}$	450	α	α	α	48.1 ± 0.3	40.0 ± 0.7	11.9 ± 0.5
			Liquid		Liquid	9.3 ± 1.0	55.5 ± 0.7	35.2 ± 0.5
14	$Ag_{15}Au_{70}Ga_{15}$	450	α	α	α	20.9 ± 0.7	68.8 ± 1.1	10.3 ± 0.5
			Liquid		Liquid	3.7 ± 0.8	70.1 ± 0.6	26.2 ± 1.2
15	$Ag_{30}Au_{50}Ga_{20}$	450	α	α	α	44.0 ± 0.5	45.9 ± 0.6	10.1 ± 0.6
			Liquid		Liquid	8.0 ± 0.8	59.3 ± 0.8	32.7 ± 0.4
16	$Ag_{20}Au_{60}Ga_{20}$	450	α	α	α	34.0 ± 0.4	56.1 ± 0.2	9.9 ± 0.3
			Liquid		Liquid	7.1 ± 2.5	63.4 ± 0.8	29.5 ± 2.1
17	$Ag_{50}Au_{20}Ga_{30}$	450	α	α	α	66.4 ± 0.3	13.5 ± 0.3	20.1 ± 0.2
			Liquid		Liquid	26.3 ± 0.8	29.0 ± 1.0	44.7 ± 0.3
18	$Ag_{20}Au_{50}Ga_{30}$	450	α	α	α	50.4 ± 0.7	36.6 ± 0.8	13.0 ± 1.0
			Liquid		Liquid	10.7 ± 1.6	52.8 ± 0.5	36.5 ± 2.0
19	$Ag_{33.3}Au_{33.3}Ga_{33.3}$	450	α	α	α	61.2 ± 0.2	21.9 ± 0.6	16.9 ± 0.6
			Liquid		Liquid	20.1 ± 1.3	39.1 ± 0.8	40.8 ± 1.1
20	$Ag_{10}Au_{50}Ga_{40}$	450	Liquid	-	Liquid	10.3 ± 1.4	49.8 ± 0.9	39.9 ± 0.6
21	$Ag_{35}Au_{10}Ga_{55}$	450	Liquid	-	Liquid	35.1 ± 0.7	9.5 ± 0.4	55.4 ± 0.5
22	$Ag_{10}Au_{30}Ga_{60}$	450	$AuGa_2$	$AuGa_2$	$AuGa_2$	-	33.5 ± 0.2	66.5 ± 0.2
			Liquid		Liquid	18.8 ± 1.6	27.0 ± 0.8	54.2 ± 1.1

Table 3. *The optimized binary parameters used in this study.*

Phase	Temperature /K	Thermodynamic parameters /J·mol^{-1}	Ref
Liquid	298.15–1234.93	${}^{0}G_{Ag}^{Liquid}$=+3815.564+109.310993·T−23.8463314·T·ln(T) − 0.001790585·T^2−3.98587×10^{-7}·T^3−12011·T^{-1}−1.033905×10^{-20}·T^7	[37]
	1234.93–3000	${}^{0}G_{Ag}^{Liquid}$=−3587.111+180.964656·T−33.472·T·ln(T)	[37]
	298.15–929.4	${}^{0}G_{Au}^{Liquid}$=+ 5613.144 + 97.444232·T−22.75455·T·ln(T) −0.00385924·T^2 + 3.79625×10^{-7}·T^3 −25097·T^{-1}	[37]
	929.4–1337.3	${}^{0}G_{Au}^{Liquid}$=-81034.481 + 1012.30956·T−155.706745·T·ln(T) +0.08756015·T^2 −1.1518713×10^{-5}·T^3 + 10637210·T^{-1}	[37]
	1337.3–1735.8	${}^{0}G_{Au}^{Liquid}$=+326619.829−2025.76412·T + 263.252259·T·ln(T) −0.118216828·T^2 + 8.923844×10^{-6}·T^3 −67999832·T^{-1}	[37]
	1735.8–3200	${}^{0}G_{Au}^{Liquid}$=+418.217 + 155.886658·T−30.9616·T·ln(T)	[37]
	200.0–302.9	${}^{0}G_{Ga}^{Liquid}$=−15821.033 +567.189696·T−108.228783·T·ln(T) +0.227155636·T^2 −1.18575257×10^{-4}·T^3 +439954·T^{-1} −7.0171×10^{-17}·T^7	[37]
	302.9–4000.0	${}^{0}G_{Ga}^{Liquid}$=-1389.188 + 114.049043·T−26.0692906·T·ln(T) +1.506×10^{-4}·T^2 −4.0173×10^{-8}·T^3 −118332·T^{-1}	[37]
		${}^{0}L_{AgAu}^{Liquid}$=-16402 + 1.14·T	[21]
		${}^{0}L_{AgGa}^{Liquid}$=-19643.799+63.659·T-8.620·T·ln(T)	[26]
		${}^{1}L_{AgGa}^{Liquid}$=-38747.760+140.716·T-16.112·T·ln(T)	[26]
		${}^{2}L_{AgGa}^{Liquid}$=-257456.683+140.455·T-17.417·T·ln(T)	[26]
		${}^{0}L_{AuGa}^{Liquid}$=-64836.418-1.669·T	[35]
		${}^{1}L_{AuGa}^{Liquid}$=-26517.288+8.315·T	[35]
		${}^{2}L_{AuGa}^{Liquid}$=-12480.212+14.248·T	[35]
FCC_A1 (Ag, Au)	298.14–3000	${}^{0}G_{Ag}^{FCC\_A1(Ag,Au)}$= +GHSERAG	[37]
	298.14–3200	${}^{0}G_{Au}^{FCC\_A1(Ag,Au)}$= +GHSERAU	[37]
		${}^{0}L_{AgAu}^{FCC\_A1(Ag,Au)}$=-15599	[21]
FCC_A1 (Ag, Ga)	298.14–3000	${}^{0}G_{Ag}^{FCC\_A1(Ag,Ga)}$= +GHSERAG	[37]
	302.91– 4000	${}^{0}G_{Ga}^{FCC\_A1(Ag,Ga)}$=-3255.643+122.53019·$T$-26.0692906·$T$·ln($T$) +1.506×10^{-4}·$T^2$-4.0173×10^{-8}·$T^3$-118332·$T^{-1}$+1.64547×10^{23}·$T^{-9}$	[37]
		${}^{0}L_{AgGa}^{FCC\_A1(Ag,Ga)}$=-19854.0434-22.306·$T$	[26]
		${}^{1}L_{AgGa}^{FCC\_A1(Ag,Ga)}$=-10412.607-22.510·$T$	[26]
ζ (HCP_A3)	298.15 –3000	${}^{0}G_{Ag}^{\zeta(HCP\_A3)}$= +GHCPAG	[37]
	298.15 –4000	${}^{0}G_{Ga}^{\zeta(HCP\_A3)}$= +GHCPGA	[37]
		${}^{0}L_{AgGa}^{\zeta(HCP\_A3)}$= -15203.295+1.786·$T$	[26]
		${}^{1}L_{AgGa}^{\zeta(HCP\_A3)}$= -22134.965+7.178·$T$	[26]
ζ'(HCP_ORD)	298.15 –3000	${}^{0}G_{Ag:Ag}^{\zeta'(HCP\_ORD)}$= 3·GHCPAG	[26]
	298.15–2000	${}^{0}G_{Ag:Ga}^{\zeta'(HCP\_ORD)}$=2·GHCPAG+GHCPGA-3.26891668×10^{4}+1.25713314×10^{1}·T	[26]
	298.15 –2000	${}^{0}G_{Ag:Va}^{\zeta'(HCP\_ORD)}$=2·GHCPAG+1.780×10^{4}	[26]
	298.15 –2000	${}^{0}L_{Ag:Ag,Ga}^{\zeta'(HCP\_ORD)}$=6368.888-14.826·$T$	[26]
	298.15 –2000	${}^{1}L_{Ag:Ag,Ga}^{\zeta'(HCP\_ORD)}$=3641.229	[26]
Ag_3Ga_2	298.15 –2000	${}^{0}G_{Ag:Ga}^{Ag_3Ga_2}$= 3·GHSERAG+2·GHSERGA - 4.96638526 + 414.6046044545·T	[26]
FCC_A1 (Au, Ga)	298.14–3200	${}^{0}G_{Au}^{FCC\_A1(Au,Ga)}$= +GHSERAU	[37]
	200.00–302.91	${}^{0}G_{Ga}^{FCC\_A1(Au,Ga)}$=-17512.331 + 575.063691·T−108.228783·T·ln(T) +0.227155636·T^2 −1.18575257×10^{-4}·T^3 + 439954·T^{-1}	[37]
	302.91–4000	${}^{0}G_{Ga}^{FCC\_A1(Au,Ga)}$=-3255.643 + 122.53019·$T$−26.0692906·$T$·ln($T$) +1.506×10^{-4}·$T^2$ −4.0173×10^{-8}·T^3 −118332·T^{-1}+1.64547×10^{23}·T^{-9}	[37]
		${}^{0}L_{AuGa}^{FCC\_A1(Au,Ga)}$=-39175.271-9.981·$T$	[35]
		${}^{1}L_{AuGa}^{FCC\_A1(Au,Ga)}$=-9422.717	[35]

Table 3 is continued on the next page.

Table 3 continues from the previous page

Orthorombic (Ga)	298.14–3200	${}^0G_{Au}^{Ort.}$=+GHSERAU+5000	[37]
	200–4000	${}^0G_{Ga}^{Ort.}$=+GHSERGA	[37]
D024		${}^0G_{Au}^{D024}$= ${}^0G_{Au}^{FCC\_A1(Au,Ga)}$+125+0.79·$T$	[38, 39]
		${}^0G_{Ga}^{D024}$= ${}^0G_{Ga}^{hcp}$= ${}^0G_{Ga}^{Ort.}$+4500-9.5·T	[37]
		${}^0L^{D024}$=-41254.465-10.662·T	[35]
		${}^1L^{D024}$=-14732.616	[35]
βAu_7Ga_2		${}^0G_m^{\beta Au_7Ga_2}$=0.78950· ${}^0G_{Au}^{FCC\_A1(Au,Ga)}$+0.21050· ${}^0G_{Ga}^{Ort.}$-10903.861-2.673·T	[35]
$\beta' Au_7Ga_2$		${}^0G_m^{\beta' Au_7Ga_2}$=0.77770· ${}^0G_{Au}^{FCC\_A1(Au,Ga)}$+0.22230· ${}^0G_{Ga}^{Ort.}$-12318.231-1.276·T	[35]
γAu_7Ga_2		${}^0G_m^{\gamma Au_7Ga_3}$=0.70· ${}^0G_{Au}^{FCC\_A1(Au,Ga)}$+0.30· ${}^0G_{Ga}^{Ort.}$-16793.819+1.314·T	[35]
AuGa		${}^0G_m^{AuGa}$=0.50· ${}^0G_{Au}^{FCC\_A1(Au,Ga)}$+0.50· ${}^0G_{Ga}^{Ort.}$-20815.031-1.528·T	[35]
$AuGa_2$		${}^0G_m^{AuGa_2}$=0.3333· ${}^0G_{Au}^{FCC\_A1(Au,Ga)}$+0.6667· ${}^0G_{Ga}^{Ort.}$-21839.222+0.778·T	[35]
GHSERAG	298.15–1234.93	-7209.512+118.202013·T-23.8463314·T·ln(T) -0.001790585·T^2-3.98587×10^{-7}·T^3-12011·T^{-1}	[37]
	1234.93–3000	−15095.252 + 190.266404·T−33.472·T·ln(T) + 1.411773 + 29·T^{-9}	[37]
GHSERAU	298.15–929.4	-6938.856+106.830098·T-22.75455·T·ln(T) -3.85924·T^2+0.37962×10^{-6}·T^3-25097·T^{-1}	[37]
	929.40–1337.3	-93586.481+1021.69543·T-155.7067449·T·ln(T) +87.56015×10^{-3}·T^2-11.518713×10^{-6}·T^3+10637210·T^{-1}	[37]
	1337.30–1735.8	+314067.829-2016.378254·T+263.2522592·T·ln(T) -118.216828×10^{-3}·T^2+8.923844×10^{-6}·T^3-67999832·T^{-1}	[37]
	1735.80–3200	-12133.783+165.272524·T-30.9616·T·ln(T)	[37]
GHSERGA	200.00–302.9	-21312.331+585.263691·T-108.2287832·T·ln(T) +227.155636×10^{-3}·T^2-118.575257×10^{-6}·T^3+439954·T^{-1}	[37]
	302.90–4000	-7055.643+132.73019·T-26.0692906·T·ln(T) +0.1506×10^{-3}·T^{-2}-0.040173×10^{-6}·T^3-118332·T^{-1}+1.64547×10^{23}·T^{-9}	[37]
GHCPAG	298.15 –1234.93	−6909.512 + 118.502013·T−23.8463314·T·ln(T) −0.001790585·T^2−3.98587×10^{-7}·T^3−12011·T^{-1}	[37]
	1234.93– 3000	−14795.252 + 190.566404·T−33.472·T·ln(T) + 1.411773·10^{29}·T^{-9}	[37]
GHCPGA	200.00 –302.91	−16812.331 + 575.763691·T−108.228783·T·ln(T) +0 .227155636·T^2−1.18575257×10^{-4}·T^3 + 439954·T^{-1}	[37]
	302.91–4000.00	−2555.643 + 123.23019·T−26.0692906·T·ln(T) + 1.506·10^{-4}·T^2 −4.0173×10^{-8}·T^3 −118332·T^{-1} + 1.64547×10^{23}·T^{-9}	[37]

The predicted isothermal section at 450 °C compared with experimental results from this work is shown in Fig. 4. On the basis of results presented in Table 2 the following fields are determined: two-phase regions: [α+ liquid, $AuGa_2$+liquid] and one-phase region a. Ternary solubilities are again insignificant in binary compound $AuGa_2$, except for solid solubility of 20.1 at.% of Ga in a phase.

The experimentally detected phases (XRD) and their compositions (SEM/EDS) in the studied alloys (Table 2) confirm the results of thermodynamic predictions (Fig. 3 and 4). There are some small discrepancies in the phases chemical composition derived from experiments and from prediction. This differences can be explained that the prediction bases only on binary interaction parameters and do not take into account the ternary interactions.

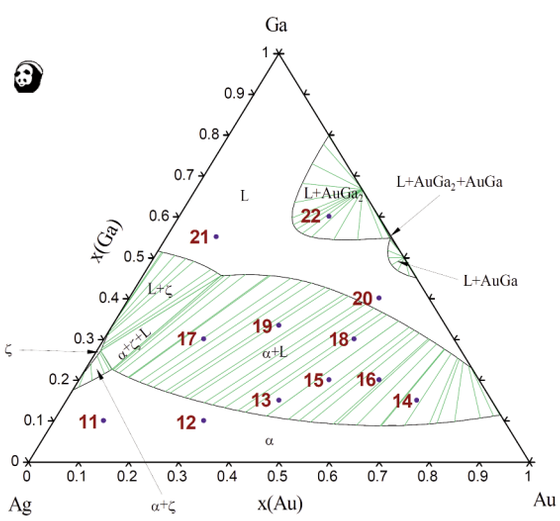

Figure 4. *Predicted isothermal section in the Ag-Au-Ga ternary system at 450 °C compared with experimental results from this work.*

5. Conclusions

To investigate the phase equilibria in the Ag-Au-Ga ternary system at 250 °C and 450 °C, the 22 alloys were studied by applying SEM/EDS and XRD analysis. Description of the isothermal sections of this ternary system (up to 70 at.% of Ga) at chosen temperatures are based on experimental data. No ternary compounds are found. Phases detected by EDS analysis are confirmed by XRD measurements. The calculated isothermal sections at 250 °C and 450 °C were found to be in a close agreement with the results of EDS and XRD analyzes (determined phases present in equilibrium field and their compositions). Experimental results obtained in present work, will be very helpful in a future optimization of the phase diagram of ternary Ag-Au-Ga system.

Acknowledgements

This work realized at AGH University of Science and Technology, Faculty of Non-Ferrous Metals under grant number IP2011020471 was supported by Polish Ministry of Science and Higher Education.

References

[1] C. Cretu, E. van der Lingen, Gold Bulletin, 32 (1999) 115-126.

[2] C.W. Corti, Blue, black and purple. The special colours of gold in: The Santa Fe Symposium. ed. E. Bell, Albuquerque: Met-Chem Research., 2004, 121-133.

[3] V.K. Bhatia, F.C. Levey, C.S. Kealley, A. Down, M.B. Cortie, Gold Bulletin, 42 (2009) 201-208.

[4] EP 0284699 S. Steinemann, Intermetallische Verbindung und ihre Verwendung 1987

[5] EP 1175515 (A1) L.P. Chuma, Jewellery alloy compositions 2002.

[6] U E. Klotz, Gold Bulletin, 43 (2010) 4-10.

[7] K. Wongpreedee, T. Tansakul, H.J. Schustere and K. Chookruvong, Purple gold: Past, present, and future to ductile intermetallics, in Gold 2006: New Industrial Applications for Gold, Limerick, Ireland (World Gold Council) 2006.

[8] J. Fischer-Bühner, A. Basso, and M. Poliero. New opportunities for blue and purple gold in jewellery casting. in: The Santa Fe Symposium. ed. E. Bell. 2009. Albuquerque, NM, USA. Met-Chem Research., 151-166.

[9] R. Schmid-Fetzer, Fundamentals of bonding by isothermal solidification for high temperature semiconductor applications, Design fundamentals of high temperature composites, intermetallics and metal–ceramic system (eds. R.Y. Lin, A. Chang, R.G. Reddy, C.T. Liu), The Minerals, Metals & Materials Society, Warrendale, PA 1995 75–98.

[10] V. M. Andronov, I.P. Grebennik, S.V. Dukarov, Functional Materials, 4 (1997) 387-391.

[11] D. Mouani, G. Morgant, B. J. Alloys Comp., 226, (1995) 222-231.

[12] H. Du, C.H. Champness, I. Shih, T. Cheung, Thin Solid Films, 480 (2005) 42–45.

[13] Y. Zhang, J.B. Li, J.K. Liang, Q. Zhang, B.J. Sun, Y.G. Xiao, G.H. Rao, J. Alloys Comp., 438 (2007) 158–164.

[14] C.A. McKay, IEEE Micro, 4 (1993) 46-58.

[15] A. A. Likhachev, K. Ullakko, Phys. Lett. A, 275 (2000) 142-151.

[16] V.V. Khovailo, V. Novosad, T. Takagi, Phys. Rev. B, 70 (2004) 174413(1)-174413(6).

[17] G. B. Brook, Gold Bulletin, 6 (1973) 8-11.

[18] P. Villars, A. Prience, H. Okamoto, Handbook of Ternary Alloy Phase Diagrams, ASM International, Metals Park, Ohio, 1995.

[19] G. Petzow, G. Effenberg, A Ternary Alloys., Comprehensive Compendium of Evaluated Constitutional Data and Phase Diagrams, Verlag Chemie, Weinheim, 1988.

[20] D. Jendrzejczyk-Handzlik, J. Chem. Thermodyn., 107 (2017) 114-125.

[21] S. Hassam, M. Gambino, M. Gaune-Escard, J.P. Bros, and J. Agren, Metall. Trans. A, 19 (1988) 409–416.

[22] H. Okamoto, J. Phase Equilib., 13 (3) (1992) 324–325.

[23] P. Feschotte, P. Bas, J. Less Common Met., 171 (1) (1991) 157–162.

[24] Y. Zhang, J.B. Li, J.K. Liang, Q.L. Liu, Y.G. Xiao, Q. Zhang, G.H. Rao, C.R. Li, Calphad, 30 (3) (2006) 316–322.

[25] Y. Zhang, Q.L. Liu, J.B. Li, J.K. Liang, J. Luo, F.S. Liu, Y.G. Xiao, G.H. Rao, J. Alloy. Compd., 399 (2005)155–159.

[26] W. Gierlotka, D. Jendrzejczyk-Handzlik, J. Alloy. Compd., 509 (2011) 38-42.

[27] ASM Handbook, vol. 3: Alloys Phase Diagrams, ASM 1998.

[28] F. Weibke, E. Hesse, Z. Anorg. Chem., 240 (1939) 289-299.

[29] C.J. Cooke, W. Hume-Rothery , J. Less-Common Met., 10 (1966) 52-56.

[30] R. P. Elliot, F. A. Shumnk, The Au-Ga (Gold-Gallium) system , Binary of Alloy Phase Equilibria , 2 (1981) 356-358.

[31] T. Massalski, H. Okamoto, Au-Ga (Gold-Gallium), Binary alloy phase diagrams in: American society for metals international, 1987.

[32] J. Liu, C. Guo, C. Li, Z. Du, J. Alloys Comp., 508 (2011) 62-70.

[33] J. Wang, Y.J. Liu, L.B. Liu, H.Y. Zhou, Z.P. Jin, Calphad, 35 (2011) 242-248.

[34] C.J. Cooke and W. Hume-Rothery, J. Less Common Met., 10 (1966) 42–51.

[35] D. Jendrzejczyk-Handzlik, J. Phase Equilib. Diffus., 38 (2017) 305–318.

[36] Pandat v. 8.1, CompuTherm LLC, 437 S. Yellowstone Dr. Suite 217 Madison,

WI 53719 USA.

[37] A.T. Dinsdale, SGTE Pure Elements (Unary) Database, Version 4.5, 2006

[38] H.S. Liu, Y. Cui, K. Ishida, and Z.P. Jin, Calphad, 27 (2003) 27–37.

[39] H.S. Liu,C.L. Liu,K. Ishida, and Z.P. Jin, J. Electron. Mater., 32 (2003) 1290–1296.